Supporting Information for "Role of Ligand Conformation on Nanoparticle-Protein Interactions"

Federica Simonelli[1], Giulia Rossi[1] and Luca Monticelli[2]**

[1] Physics Department, University of Genoa, Via Dodecaneso 33, 16146 Genoa, Italy
[2] MMSB, UMR 5086 CNRS / Universitè de Lyon, 7, Passage du Vercors, 69007 Lyon, France

NP core and ligand parameterization

We considered functionalized gold nanoparticles (AuNPs) with a diameter of about 2 nm. The core of the AuNP consisted of 144 Au atoms. The structure of the core and the binding sites of the ligands on its surface were taken from Lopez-Acevedo *et al.*[1], while the elastic network connecting the Au and S atoms were described in Torchi[2] *et al*. The surface of the Au core has 60 binding sites for sulfur atoms. To functionalize each NP, we attached 60 identical ligands to the sulfur atoms. Two different types of ligands were considered, with different hydrophobicity. The less hydrophobic ligand (referred to as Z) contained only a betaine group. The more hydrophobic ligand, indicated in the following as ZH, featured a di-butane-sulfobetaine terminal.
To parameterize the functionalized NPs we used the polarizable version of the coarse-grained Martini force field[3]. The ligands contained a hydrophobic chain of 9 CH_2 groups, which were modelled as 2 Martini C1 beads, a short chain of 4 poly-ethylene glycol monomers, represented by 4 Martini beads of type PEO (SN0 Martini type with redefined interactions according to Lee *et al.*[4] and modified angle interaction according to Bulacu *et al.*[5]) and the terminal zwitterionic group. For the PEG moieties, we also considered the latest MARTINI model by Grunewald *et al.*[6]

The parameterization of the terminal group was based on atomistic simulations by Ghobadi *et al.*[7]. We used the Martini force field to model an 8-monomer polymer containing a sulfobetaine group *per* monomer. Bead types for non-bonded interactions were chosen according to the Martini force field; the tetramethylammonium group was assigned a Q_0 type while the sulfonate ion was modeled as a Q_{da} bead. The two beads were separated by a C1 bead. For the more hydrophobic ligand two butane chains were bound to the nitrogen atom in the tetramethylammonium ion and a C1 bead was used to model each butane chain. Bonded interactions were slightly modified to match atomistic simulations. In particular, we targeted the radial distribution function (RDF) of non-bonded Q_{da} beads with respect to a Q_0 bead; we chose a Q_0 bead and computed the RDF of all Q_{da} beads (except for the one bound to the Q_0 bead). The final set of parameters is summarized in Table T1.

Table T1: Bonded interaction parameters for Z and ZH ligands. Both ligands are shown in coarse grained representation under the interaction tables. S atoms in grey, C1 beads in red, PEO

beads in orange and charged beads in yellow.

Bonds	Length [nm]	Constant [kJ mol^{-1} nm^{-2}]
S—C1	0.47	1250
C1—C1	0.47	1250
C1—PEO	0.45	5000
PEO—PEO	0.33	7000
PEO—Q_0	0.47	1250
Q_0—C1	0.40	1250
Q_0—C1 (ZH side chains)	0.47	1250
C1—Q_{da}	0.40	1250

Angles	Angle	Constant [kJ mol^{-1} rad^{-2}]
S—C1—C1	180	25
C1—C1—PEO	180	25
C1—PEO—PEO	180	25
PEO—PEO—PEO	130	CH:50 ReB:25
PEO—PEO—Q_0	180	25
PEO—Q_0—C1	180	25
PEO—Q_0—C1 (ZH side chains)	90	25
C1—Q_0—C1	180	25
Q_0—C1—Q_{da}	180	25

Dihedrals	Angle	Constant [kJ mol^{-1}]	Multiplicity
PEO—PEO—PEO—PEO	180	1.960	1
PEO—PEO—PEO—PEO	0	0.180	2
PEO—PEO—PEO—PEO	0	0.330	3
PEO—PEO—PEO—PEO	0	0.120	4

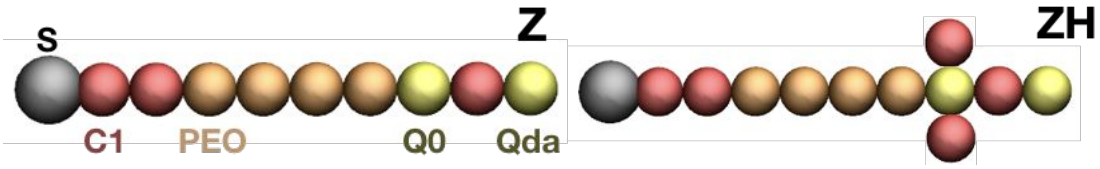

Human serum albumin parameterization

Our model of human serum albumin (HSA) is based on the crystal structure of the protein reported in the PDB with code 1ao6. Only one of the two chains was kept for parameterization. The atomistic model was obtained with the GROMACS tool *pdb2gmx*. We used the atomistic Amberff99SB-ILDN[8] force field and the TIP3P water model. The protein was inserted in a simulation box of about 12x12x12 nm^3 with physiological salt concentration (150 mM KCl). A 1.5 μs run with velocity rescale thermostat (T=310 K, τ=1 ps) and Parrinello-Rahman barostat (isotropic, p=1 atm, τ=12 ps) was performed. Positions were saved every 100 ps to have enough sampling for principal component analysis (PCA).
The coarse-grained model of HSA is based on the extension to proteins of the Martini force field[9,10]. We tested both the elastic network and the Elnedyn[11] versions of the force field. We considered only the standard parameters for the elastic network while for the Elnedyn version we varied both backbone (k_{BB}) and elastic network (k_{el}) constants. We ran a 2 μs simulation for each coarse-grained model and compared the results with the atomistic model in terms of root mean square deviation (RMSD), root mean square fluctuations (RMSF), and PCA. To establish the best agreement with the atomistic model we use also the RMSIP index, that is the root meat squared inner product of the principal components (PCs). We consider only the first 20 PCs. The best set of parameters was: k_{BB}=90000 kJ $mol^{-1}nm^{-2}$, k_{el}=350 kJ $mol^{-1}nm^{-2}$, cutoff distance=0.9 nm.

Simulation details

We performed molecular dynamics simulations in explicit polarizable water and at physiological salt concentration. For the zwitterionic NPs, we ran 20 simulations for each kind of NP. The initial configuration of these simulations was obtained by rotating the protein with respect to the NP which was kept in the same position in each initial configuration. One NP and one HSA were inserted in a simulation box of about 20x20x20 nm^3. Minimization and equilibration runs were performed before the simulation run. Each equilibration run was 20 ns long. Production runs were 3 μs long, each, for each NP and were performed with the velocity rescale thermostat[12] (T=310 K, τ=1 ps) and Parrinello-Rahman barostat[13] (isotropic, p=1 atm, τ=12 ps).
We performed 5 additional simulations with the PEG model by Grunewald, using the same setup as above and the same simulation parameters. No differences in the behavior of the 2 kinds of NPs were observed.

PEG ligands

We performed 2 simulations of a single NP covered by 60 PEG ligands. Each ligand consisted of 9 monomers, i.e., the same number of beads as in the zwitterionic Z ligand. Each production run was 3 μs long. The same parameters and initial configuration setup were used in the simulations.
The number of contacts between the PEGylated NP and HSA within 0.8 nm is shown as a function of time in figure S1 for the 2 simulation runs. Raw data are smoothed with a moving average algorithm (50 points in each averaging window). In both simulations, once the NP-protein contact was established, it remained stable throughout the simulation (3 μs).

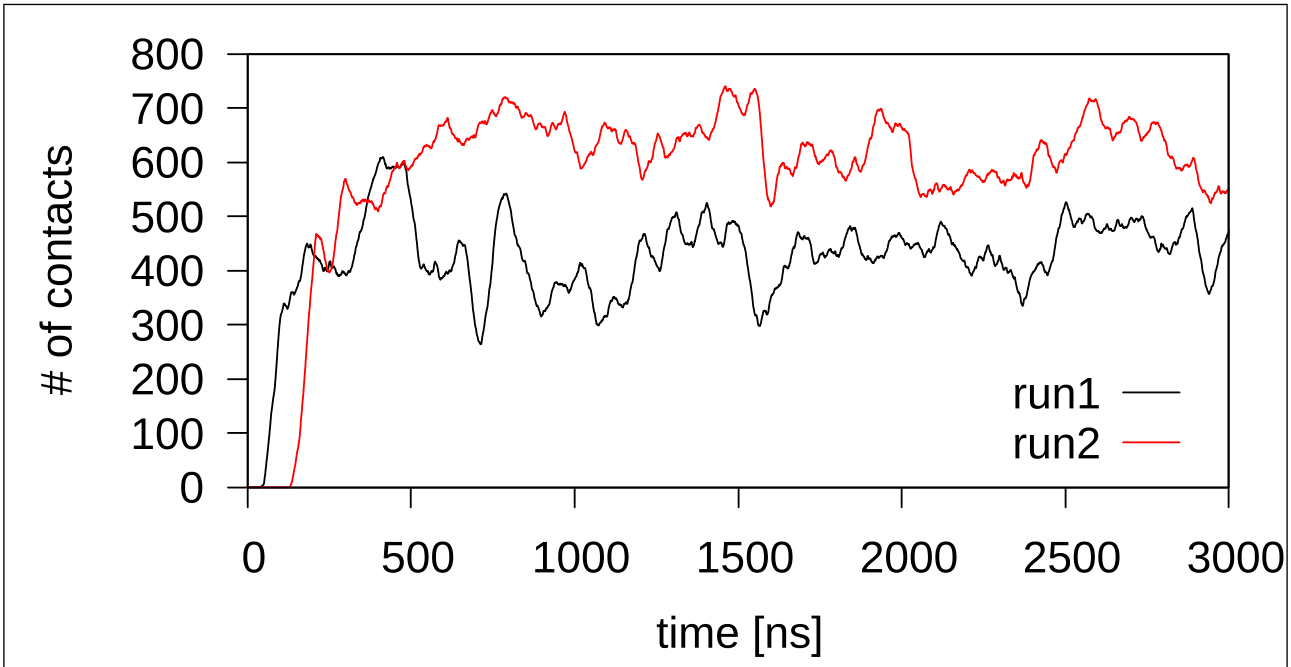

Figure S1: The number of contacts between the PEGylated NP and HSA is plotted as a function of time. Both simulation runs are shown.

Classification of protein residues

Amino acids can be divided in charged, polar and hydrophobic (https://proteinstructures.com/Structure/Structure/amino-acids.html). Based on this classification, the residues in HSA are grouped to compute the number of contacts for different residue characters. Once divided by character, residues were grouped in surface and core residues according to their solvent accessible surface area (SASA). The SASA for each residue was computed from protein simulations in polarizable water using the GROMACS tool *gmx sasa*. A maximum value of SASA was then assigned to each amino acid according to Tien *et al.*[14]. The relative surface area, that is the ratio between the SASA and its maximum value for each residue, was used to discriminate between surface and core residues. If the ratio was below a threshold of 0.2, residues were considered as core residues, otherwise as surface residues. Only surface residues were considered in the calculation of the number of contacts.

NP-protein contacts

The average number of contacts was computed as follow: first, the number of contacts between the NP and different groups of residues in the protein was computed as a function of time for each simulation; then an average over all simulations was computed, using the GROMACS tool *gmx analyze*. The average for each group was divided by the number of beads in the group. Final results were given as percentage of the total number of contacts.

Water-NP contacts

The number of contacts between water and the 2 NPs were computed in two regimes: presence of NP-protein contacts and absence of NP-protein contacts. To determine the presence of a contact, a threshold of 0.8 nm was used (distance between NP and protein beads). The average number of contacts was computed considering all the stretches of contact/non-contact for the 20 simulations with the GROMACS tool *gmx analyze*. Only the W bead (the only one with Van der Waals interactions) of polarizable water was considered for contacts.

References

(1) Lopez-Acevedo, O.; Akola, J.; Whetten, R. L.; Grönbeck, H.; Häkkinen, H. Structure and Bonding in the Ubiquitous Icosahedral Metallic Gold Cluster Au 144(SR) 60. *J. Phys. Chem. C* **2009**, *113*, 5035–5038.

(2) Torchi, A.; Simonelli, F.; Ferrando, R.; Rossi, G. Local Enhancement of Lipid Membrane Permeability Induced by Irradiated Gold Nanoparticles. *ACS Nano* **2017**, *11*, 12553–12561.

(3) Yesylevskyy, S. O.; Schäfer, L. V; Sengupta, D.; Marrink, S. J. Polarizable Water Model for the Coarse-Grained MARTINI Force Field. *PLoS Comput. Biol.* **2010**, *6*, e1000810.

(4) Lee, H.; Pastor, R. W. Coarse-Grained Model for PEGylated Lipids: Effect of PEGylation on the Size and Shape of Self-Assembled Structures. *J. Phys. Chem. B* **2011**, *115*, 7830–7837.

(5) Bulacu, M.; Goga, N.; Zhao, W.; Rossi, G.; Monticelli, L.; Periole, X.; Tieleman, D. P.; Marrink, S. J. Improved Angle Potentials for Coarse-Grained Molecular Dynamics Simulations. *J. Chem. Theory Comput.* **2013**, *9*, 3282–3292.

(6) Grunewald, F.; Rossi, G.; De Vries, A. H.; Marrink, S. J.; Monticelli, L. A Transferable MARTINI Model of Polyethylene Oxide. *J. Phys. Chem. B* **2018**, *122*, 7436–7449.

(7) Ghobadi, A. F.; Letteri, R.; Parelkar, S. S.; Zhao, Y.; Chan-Seng, D.; Emrick, T.; Jayaraman, A. Dispersing Zwitterions into Comb Polymers for Nonviral Transfection: Experiments and Molecular Simulation. *Biomacromolecules* **2016**, *17*, 546–557.

(8) Lindorff-Larsen, K.; Piana, S.; Palmo, K.; Maragakis, P.; Klepeis, J. L.; Dror, R. O.; Shaw, D. E. Improved Side-Chain Torsion Potentials for the Amber Ff99SB Protein Force Field. *Proteins Struct. Funct. Bioinforma.* **2010**, *78*, 1950–1958.

(9) Monticelli, L.; Kandasamy, S. K.; Periole, X.; Larson, R. G.; Tieleman, D. P.; Marrink, S. J. The MARTINI Coarse Grained Force Field: Extension to Proteins. *J. Chem. Theory Comput.* **2008**, *4*, 819–834.

(10) Jong, D. H. De; Singh, G.; Bennett, W. F. D.; Wassenaar, T. a; Sch, L. V; Periole, X.; Tieleman, P.; Marrink, S. J. Improved Parameters For F or The Martini Coarse- Coarse - Grained Protein Force Field. *J. Chem. Theory Comput.* **2012**, *9*, 687–697.

(11) Periole, X.; Cavalli, M.; Marrink, S.-J.; Ceruso, M. a. Combining an Elastic Network With a Coarse-Grained Molecular Force Field: Structure, Dynamics, and Intermolecular Recognition. *J. Chem. Theory Comput.* **2009**, *5*, 2531–2543.

(12) Bussi, G.; Donadio, D.; Parrinello, M. Canonical Sampling through Velocity Rescaling. *J. Chem. Phys.* **2007**, *126*, 014101.

(13) Parrinello, M.; Rahman, A. Polymorphic Transitions in Single Crystals: A New Molecular Dynamics Method. *J. Appl. Phys.* **1981**, *52*, 7182.

(14) Tien, M. Z.; Meyer, A. G.; Sydykova, D. K.; Spielman, S. J.; Wilke, C. O. Maximum Allowed Solvent Accessibilites of Residues in Proteins. *PLoS One* **2013**, *8*.